Journal of Molecular Graphics and Modelling xxx (2015) xxx–xxx

Contents lists available at ScienceDirect

Journal of Molecular Graphics and Modelling

journal homepage: www.elsevier.com/locate/JMGM

Layered SiC sheets: A promising metal-free catalyst for NO reduction

Jing wen Feng, Yue jie Liu, Jing xiang Zhao *

College of Chemistry and Chemical Engineering, Harbin Normal University, Harbin, 150025, People's Republic of China

ARTICLE INFO

Article history:
Received 5 January 2015
Received in revised form 1 May 2015
Accepted 5 May 2015
Available online 12 May 2015

Keywords:
Layered SiC sheets
NO reduction
DFT
Dimer mechanism
Metal-free

ABSTRACT

Recently, the catalytic reduction is shown to be an effective method to remove the harmful NO. In terms of the high cost and limited supply of the traditional transition metal-based catalysts, the novel metal-free catalyst is highly desirable for NO reduction. Here, density functional theory (DFT) computations were performed to explore the potentials of layered SiC sheets as a metal-free catalyst for NO reduction. From our DFT results, it can be predicted that layered SiC sheets exhibit superior catalytic activity toward NO reduction. In particular, a dimer mechanism is shown to be more favorable than the direct dissociation one for NO reduction on this metal-free catalyst and a three-step mechanism is involved in this process: (1) the formation of a $(NO)_2$ dimer on layered SiC sheet, followed by (2) its dissociation into $N_2O + O_{ad}$, and (3) the recovery of catalyst by subsequent NO. The trans-$(NO)_2$ dimer might be a necessary intermediate, in which the calculated barrier for the rate-determining step along the energetically most favorable pathway is 0.722 eV. The high reactivity of layered SiC sheets may be attributed to the certain amount of charge transfer from the catalyst to $(NO)_2$ dimer, which shortens the N—N bonding and thus stabilizes these systems due to the extra electrons on the dimers. This excellent catalytic activity provides a useful guidance to design the next generation catalysts for NO reduction with lower cost and higher activity.

1. Introduction

NO reduction plays an important role in solving the growing environmental problems caused by NO emission from fuel combustion, industrial processes, and so on [1]. Earlier investigations, both experimentally and theoretically, have shown that transition metal-based catalysts have conventionally been employed for NO reduction due to their high activity [2–25]. For example, some noble metals of Ir [23], Pd [9], Ag [24], and Au [25] etc. can effectively catalyze NO reduction. However, the high cost and limited supply hinder their large-scale commercialization to a certain extent. To overcome this problem, recent studies have been devoted to address alternative catalysts such as alloys [26,27], metal oxides [28–30], carbon nanotube-supported metal particles [31,32], and zeolites [33,34].

Carbon-based catalysts are expected to be the most promising alternatives to transition metal-based catalysts because C is more abundant and durable, as well as cheap. Interestingly, the introduction of non carbon (such as B, N, Si, P, S) atoms into the hexagonal carbon frameworks of graphenes or carbon nanotubes is generally effective in tuning their electrical properties and chemical activities [35,36]. For example, both experimental and theoretical studies have reported that doped carbon materials are promising candidates to replace Pt-based catalysts for fuel cells owing to their high catalytic activity, long-term stability, and excellent CO tolerance [37–43]. Encouraged by these studies, our earlier study suggests that Si-doped graphene is an effective and metal-free catalyst for CO oxidation [44] or NO reduction [45]. However, the low dopant concentration in carbon–based catalysts limits the improvement of their catalytic activity (N ~ 4–6 at%, B ~ 0–2.24 at%, and 1–2 at% of S) [39–41]. For practical applications, catalysts with a large active region are highly desired for NO reduction.

SiC-based nanocomposites exhibit high saturated carrier mobility, high critical electrical field, and high thermal conductivity. Recently, a planar phase of SiC with sp^2-hybridized feature resembling graphene was theoretically shown to exhibit high structural stability [46], and its corresponding electronic properties have been reported by Zhou et al. [47,48]. In addition, Li et al. also reported a unique phase SiC_2 silagraphene, in which each Si atom is bonded with four C atoms, while each C atom is bonded with two Si atoms [49]. The most interesting is that graphene-like SiC sheet can provide more active reaction sites than present doped carbon materials. For example, layered SiC sheets can serve as a feasible metal-free oxygen reduction reaction electrocatalyst [50]. Since layered SiC sheet possess high chemical reactivity, we highly wonder whether it can be used as a potential candidate as the metal-free

* Corresponding author. Tel.: +86 45188060580; fax: +86 45188060580..
E-mail addresses: zhaojingxiang@hrbnu.edu.cn, xjz_hmily@163.com (J.x. Zhao).

http://dx.doi.org/10.1016/j.jmgm.2015.05.002
1093-3263/

catalyst for NO reduction. In particular, it was found that the NO molecule on SiC-based materials create strong Si—N bonds, which might initiate NO reduction [51]. Hence, in this work, we would carry out density functional theory (DFT) calculations to investigate this above issue, which may be helpful to fabricate novel and metal-free NO reduction catalysts.

2. Computational details

All calculations were performed within spin-polarized DFT framework, which are implemented in the DMol^3 code [52,53]. The generalized gradient approximation (GGA) with the Perdew–Burke–Ernzerhof (PBE) exchange-correlation functional was used to describe exchange and correlation effects [54], which is the most common density functional in materials and surface science. The double numerical basis sets with polarization functions (DNP) was chosen as the basis set, whose accuracy is comparable to a Gaussian 6–31 (d) basis and exhibit excellent consistency with experiments. In addition, we also compared the present results with those calculated using triple numerical plus polarization (TNP), as shown in Table S1 in Supporting Information. We find that the adsorption energies based on TNP are slightly larger than those of based on DNP. During the structural optimization, no symmetry constraints were imposed. The convergence tolerance of energy is 10^{-5} Ha, maximum force is 0.001 Ha/Å, and maximum displacement is 0.005 Å in the geometry optimization. Moreover, in order to ensure high quality results, the real space global orbital cutoff radius is set as high as 4.6 Å and the smearing of electronic occupations is 0.005 Ha. The Hirshfeld method [55] was adopted to calculate the charge transfer.

For layered SiC sheets, we employed a hexagonal supercell (5×5 graphene unit cells) according to the unit cell tests as shown in Table S2. Notably, Jiang et al. have recently suggested that the layered SiC sheets are shown to be energetically favorable than cubic ones when the layer number is less than 4 [50]. To avoid the interaction of layered SiC sheet and its periodic image, we set the modulus unit cell vector in the z direction to be as large as 15 Å according to test as shown in Table S3. The $3 \times 3 \times 1$ k points were used for calculating the Brillouin zone integration. The linear synchronous transit (LST/QST) tools in Dmol^3 code were used to obtain the transition state [56].

3. Results and discussion

3.1. The adsorption of $(NO)_n$ (n = 1 or 2) on layered SiC sheet

Two possible mechanisms for NO reduction to N_2O have been proposed in the previous studies [10–13,57–59], i.e., direct dissociation mechanism [57–59] and the dimer mechanism [10–13]. In the former, an adsorbed NO molecule first dissociates into N and O atoms, and then another NO molecule associates the N atom to release a N_2O molecule. In the latter, two NO molecule initially couple into a $(NO)_2$ dimer, followed by the dissociation into a N_2O molecule and O atom. It is well known that the initial adsorption manner of a molecule on the catalyst surface can greatly affects the subsequent surface reactions. To better gain insight into the catalytic reactivity of layered SiC sheet toward NO molecules, the adsorption of NO monomer and dimer on SiC sheet is firstly explored. Their adsorption energies are determined by $E_{ad} = E_{ads/SiC} - E_{ads} - E_{SiC}$, where $E_{ads/SiC}$, E_{ads}, and E_{SiC} are the total energies of the adsorption systems, the isolated adsorbate

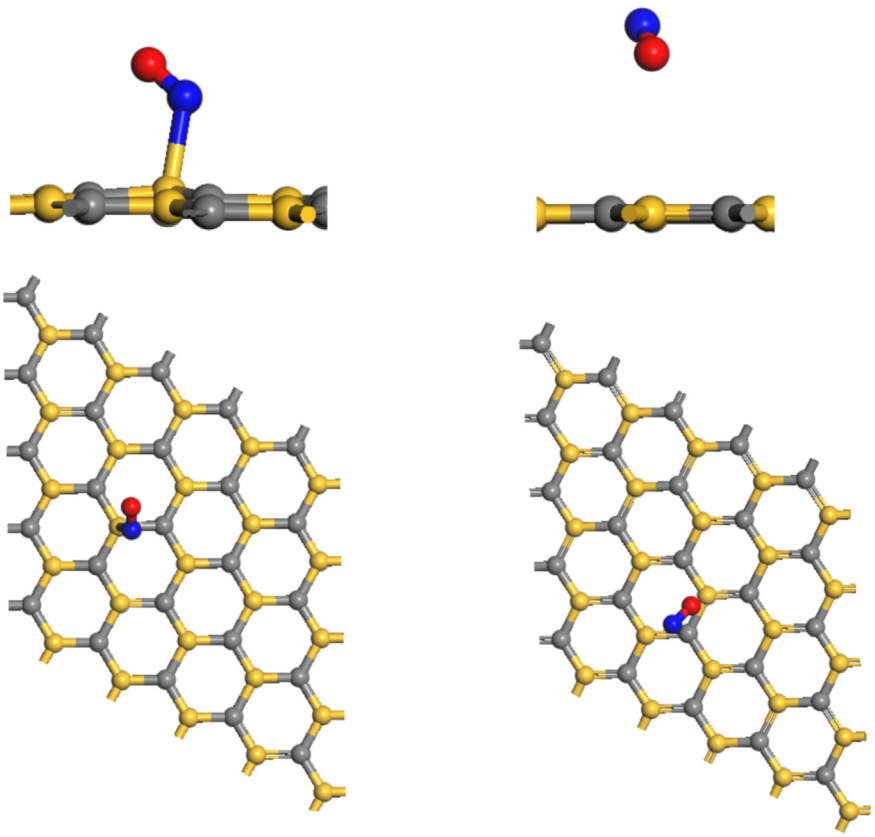

Fig. 1. Optimized geometric structures of NO monomer on layered SiC sheet: (a) N_{ad}-geometry and (b) O_{ad}-geometry.

Please cite this article in press as: J.w. Feng, et al., Layered SiC sheets: A promising metal-free catalyst for NO reduction, J. Mol. Graph. Model. (2015), http://dx.doi.org/10.1016/j.jmgm.2015.05.002

molecule, and the layered SiC sheets, respectively. Negative adsorption energies correspond to exothermic adsorption processes, while positive adsorption energies do endothermic ones.

For the adsorption of NO monomer on SiC sheet, several possible high symmetry adsorption sites are considered, including the top, bridge, and hollow sites. The stable adsorption structures and energies of NO monomer are shown in Fig. 1. It is found that the most energetically favorable site for NO monomer adsorption on the single-layer SiC is characterized by NO titled with the SiC surface (Fig. 1a) with adsorption energy of −0.118 eV, which is much smaller than that of Si-doped graphene (−0.809 eV). The length of the newly formed Si—N bond is 2.204 Å. The small adsorption energy and large distance between NO and SiC sheet suggest that monomer NO molecule can be weakly adsorbed on the layered SiC sheets. Moreover, the N—O bond is elongated by ∼0.01 Å, accompanying with a negligible charge transfer from SiC to the $2\pi^*$ orbital of NO (0.08 *e*). In addition, a meta-stable configuration is also obtained as shown in Fig. 1b with adsorption energy of −0.069 eV, in which the O atom of NO molecule is attached to the Si site with distance of 3.587 Å.

Considering that the $(NO)_2$ dimer may be a necessary intermediate in the process of NO reduction on catalysts surface, we next investigate the adsorption of $(NO)_2$ dimer on layered SiC sheet. In fact, Dinerman et al. had characterized the structure of gas-phase $(NO)_2$ dimer via infrared spectroscopy in 1970 [60]. Three initial configurations are examined for the interaction between $(NO)_2$ dimer and layered SiC sheet, i.e., the two NO molecules are preadsorbed with two O atoms, two N atoms, or the O atom of a molecule and the N atom of the other molecule close to the surface. After fully structural relaxation, five dimers are obtained as shown in Fig. 2, which are denoted as D_n ($n = 1 \sim 5$) for simplicity. The corresponding structural parameters are presented in Table 1. Similar to the case of on Si-doped graphene, the NO molecules in the five adsorbed dimers are connected to each other via a N—N bond of 1.281 (for D_1), 1.242 (for D_2), 1.357 (for D_3), 1.362 (for D_4), and 1.286 Å (for D_5), which are much shorter than that of the gas phase $(NO)_2$ dimer (1.970 Å). Moreover, the adsorption energies of the five dimers range from −1.593 (D_1) to −0.478 eV (D_5), which are at least four times as large as that of the NO monomer (E_{ad} = −0.118 eV). Notably, the adsorption energies of $(NO)_2$ dimer on SiC sheet are nearly independent on the layers of SiC sheet as shown in Table S4. Due to the spin couple, the dimer is spin nonpolarized, while the NO monomer adsorption on layered SiC sheet is spin-polarized.

Structure D_1 (Fig. 2a) is a zigzag $O_{ad}NN_{ad}O_{ad}$ species, in which the two O atoms of dimer are adsorbed on the two neighboring Si atoms in the same hexagonal Si_3C_3 ring, while one N atom is attached to the neighboring C atom of substarte. The distances of the formed Si_1—O_1, Si_2—O_2, and N_1—C are 1.866, 1.873, and 1.484 Å, respectively, while the two N—O bond lengths are 1.333 and 1.354 Å, as shown in Table 1a. We should point out that this dimer originates from structure I where the O atom of one NO molecule and the N atom of the other NO molecule initially interact with the layered SiC sheet. It can be obviously seen from Fig. 3a that structure I is more stable by 0.156 eV than the two free NO molecules and the conversion from structure I into D_1 easily occur due to a small barrier of 0.085 eV (TS1).

Structure D_2 (Fig. 2b) is characterized as a trapezoid $O_{ad}NNO_{ad}$ complex, in which the shortest distance between $(NO)_2$ dimer and SiC sheet is 1.751 Å (Table 1b). In particular, structure D_2 can be easily obtained when two NO molecules approach to two Si atoms in the same hexagonal ring of the SiC sheet with their O atoms, i.e., structure II. As shown in Fig. 3b, structure II is energetically more stable than the separated reactants by 0.458 eV. Moreover, the energy barrier from structure II to D_2 is 0.722 eV and the involved transition state is TS2.

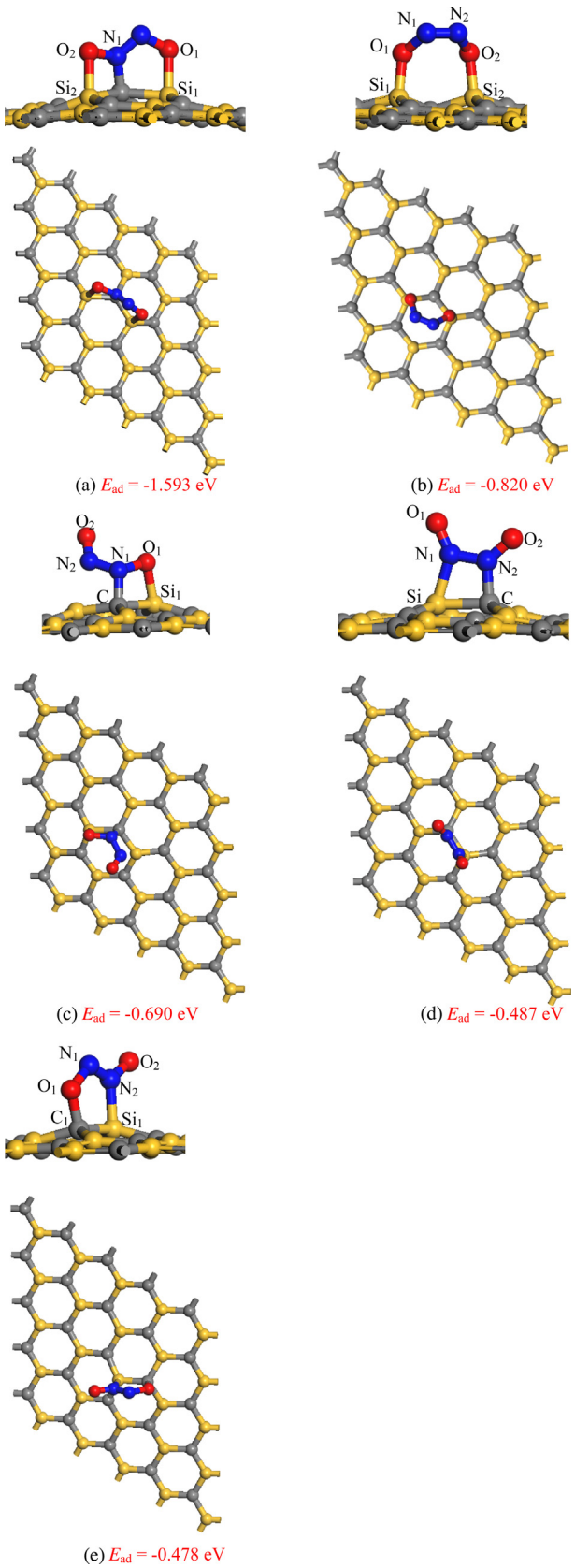

Fig. 2. Optimized geometric structures of $(NO)_2$ dimer on layered SiC sheet: (a) D_1, (b) D_2, (c) D_3, (d) D_4, and (e) D_5.

Please cite this article in press as: J.w. Feng, et al., Layered SiC sheets: A promising metal-free catalyst for NO reduction, J. Mol. Graph. Model. (2015), http://dx.doi.org/10.1016/j.jmgm.2015.05.002

Table 1
Structural parameters for the intermediate states along various minimum energy pathways (a) I, (b) II, (c) III, (d) IV, and (e) V for the NO reduction on the layered SiC sheet. The unit of the bond length is Å.

(a)

Path I	I	TS1	D_1	TS1a	FS
$d_{O_2-Si_2}$	3.925	3.395	1.873	2.073	3.673
$d_{O_2-N_1}$	1.162	1.183	1.354	1.298	1.196
$d_{N_1-N_2}$	2.852	1.760	1.281	1.169	1.140
d_{N_1-C}	–	2.776	1.484	2.186	3.903
$d_{N_2-O_1}$	1.163	1.192	1.333	1.894	3.494
$d_{O_1-Si_1}$	–	2.894	1.866	1.668	1.690

(b)

Path II	II	TS2	D_2	TS2a	FS
$d_{O_1-Si_1}$	3.781	2.426	1.753	2.253	3.935
$d_{O_1-N_1}$	1.168	1.239	1.411	1.243	1.196
$d_{N_1-N_2}$	2.017	1.505	1.243	1.161	1.139
$d_{N_2-O_2}$	1.168	1.231	1.413	2.014	3.202
$d_{O_2-Si_2}$	3.781	2.460	1.751	1.650	1.620

(c)

Path III	III	D_3	TS3
$d_{O_1-Si_1}$	1.781	1.825	1.751
$d_{O_1-N_1}$	1.384	1.394	1.440
$d_{N_1-N_2}$	4.400	1.357	1.809
d_{N_1-C}	1.536	1.501	1.525
$d_{N_2-O_2}$	1.165	1.219	1.169

(d)

Path IV	IV	TS4	D_4	TS4a	FS
d_{N_1-Si}	4.010	2.595	1.895	–	–
$d_{N_1-O_1}$	1.168	1.206	1.242	1.265	3.285
$d_{N_1-N_2}$	2.025	1.587	1.362	1.331	1.139
$d_{N_2-O_2}$	1.169	1.199	1.246	1.284	1.196
d_{N_2-C}	3.638	2.357	1.560	–	–

(e)

Path V	V	TS5	D_5	TS5a	FS
$d_{O_1-C_1}$	3.985	2.525	1.581	1.466	1.530
$d_{O_1-N_1}$	1.169	1.210	1.400	1.932	3.198
$d_{N_1-N_2}$	1.997	1.512	1.286	1.205	1.139
$d_{N_2-O_2}$	1.169	1.215	1.262	1.257	1.197
$d_{N_2-Si_1}$	3.251	2.410	1.914	2.253	4.043

For structure D_3 (Fig. 2c) and D_4 (Fig. 2d), they contain an adsorbed cis-$(NO)_2$ species on the SiC sheet. In the former, the lengths of N_1—C and O_1—Si_1 bonds are 1.501 and 1.825 Å, while the N_1—Si_1 and N_2—C bond lengths in the latter are 1.895 and 1.560 Å, respectively. Moreover, the origin of the two structures is greatly different: (i) D_3 comes from the structure III, which lies below the reaction entrance by 0.172 eV as presented in Fig. 3c. In structure III, one NO molecule is first attached on SiC sheet and a second NO molecule is adsorbed, leading to the formation of a N—N bond. Due to the spin couple, structure III can transform into D_3 without any energy barrier. For D_4, it originates from structure IV, in which two NO molecules employ their respective N atoms to attack to one of Si—C bond of SiC sheet. Structure IV and D_4 are connected by the TS4, whose is less energetically favorable than structure IV by 0.645 eV (Fig. 3d).

Structure D_5 is a zigzag $O_{ad}NN_{ad}O$ species and the newly formed O_1—C_1 and N_2—Si_1 bond lengths are 1.581 and 1.914 Å. Initially, the O_1 atom of the first NO is close to the C_1 atom of SiC sheet, while the N_2 atom of the second NO approaches to the Si_1 atom, leading to the formation of structure V. This intermediate lies below the reaction entrance by 0.439 eV as presented in Fig. 3e. Along the reaction coordination, structure V evolves into D_5 via TS5 with a barrier of 0.276 eV. Finally, we should point out that structure I, II, III, IV, and V exhibit a triplet state.

3.2. The formation of N_2O

As discussed above, there are two well established reaction mechanisms, i.e., direct dissociation and dimer mechanism, for NO reduction. As follows, we would address the two involved mechanisms for NO reduction on the layered SiC sheet:

3.2.1. Direct dissociation mechanism

The most stable adsorption configuration of NO monomer on SiC sheet (Fig. 1a) is adopted as the initial state (IS), while the final state (FS) is that the N and O atoms are coadsorbed on the SiC sheet. To achieve sufficient accuracy, 20 image structures were inserted between IS and FS. The calculated minimum energy pathway (MEP) profile is given in Fig. 4, where the sum of the energies of SiC sheet and the separate NO monomer is set as the reference energy. As seen from Fig. 4, a late transition state (TS_a) with a high barrier of 2.857 eV has to overcome in this process. Meanwhile, the FS is energetically less favorable than IS by 0.222 eV. In other words, it is very difficult for NO monomer to directly dissociate on SiC sheet

Please cite this article in press as: J.w. Feng, et al., Layered SiC sheets: A promising metal-free catalyst for NO reduction, J. Mol. Graph. Model. (2015), http://dx.doi.org/10.1016/j.jmgm.2015.05.002

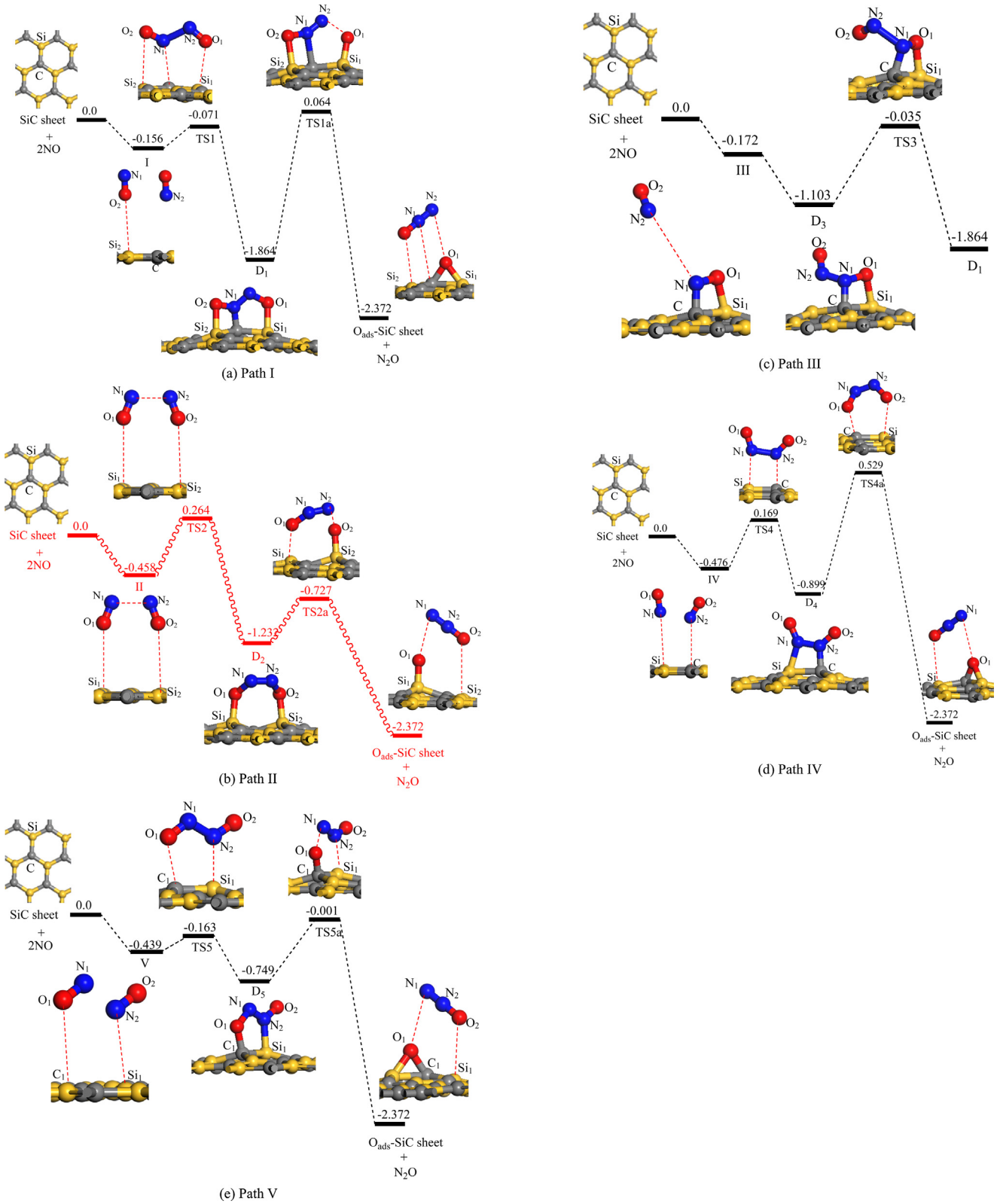

Fig. 3. The MEP profile with the optimized geometries of intermediates, transition states, and products for NO reduction on layered SiC sheet along various pathways: (a) path I, (b) path II, (c) path III, (d) path IV, and (e) path V. The unit of the energy is eV. The electronic energies of pristine SiC layers plus two isolated NO molecules are taken as zero for reference.

due to the high barrier and endothermicity of this reaction, which is similar to the case on Si doped graphene [45]. We thus expect that the reduction from NO to N_2O does not occur on this catalyst through the direct dissociation mechanism.

3.2.2. Dimer mechanism

In Fig. 3, we present the MEP profiles of the dimer mechanism, the corresponding intermediates, and transition states. Their structural parameters are summarized in Table 1. As shown in

Please cite this article in press as: J.w. Feng, et al., Layered SiC sheets: A promising metal-free catalyst for NO reduction, J. Mol. Graph. Model. (2015), http://dx.doi.org/10.1016/j.jmgm.2015.05.002

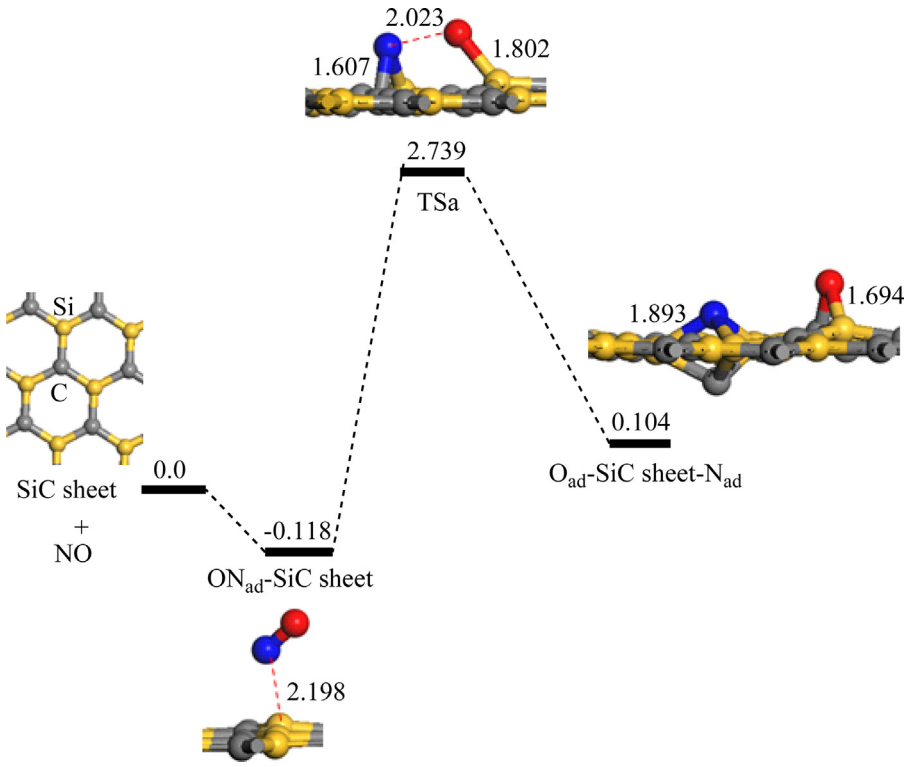

Fig. 4. The MEP profile with the optimized geometries of intermediates, transition states, and products for NO direct dissociation on layered SiC sheet. The units of the bond length and energy are Å and eV.

Fig. 3a, structure D_1 can be directly converted into the product (P, $N_2O + O_{ads}$) through a transition state (TS1a) with a high energy barrier of 1.928 eV. Compared to D_1, the Si_2—O_2, N_1—C, and N_2—O_1 bonds in TS1a are elongated to 2.073, 2.186, and 1.894 Å, respectively, while the Si_1—O_1 bond is shortened to 1.668 Å. Moreover, the reaction of $D_1 \rightarrow P$ is exothermic by 0.508 eV. For structure D_2, it can also transform into N_2O, leaving an oxygen atom on SiC sheet. The energy barrier and released energy for this step are 0.505 and 1.140 eV (Fig. 3b). Compared to D_2, the Si_1—O_1 bond in the involved transition state (TS2a) is elongated by 0.500 Å. For structure D_3, it is first transformed into structure D_1 with an energy barrier of 1.068 eV (TS3) and the exothermicity of this process is 0.761 eV (Fig. 3c). Finally, structure D_4 and D_5 are converted into N_2O through TS4a and TS5a with the barriers of 1.428 and 0.748 eV as presented in Fig. 3d and e. The released energies in the two steps are 1.473 and 1.623 eV. It should be pointed out that the formed N_2O is easily escapes from the SiC sheet due to the weak interaction between each other (E_{ads} = ~−0.07 eV).

In general, the overall barrier in a catalysis process is more important than a single step barrier. If one intermediate reaction is endothermic, the overall barrier can be higher than that of all the single steps. On the contrary, the overall barrier should be the barrier of the highest single step. In the present work, both the intermediates and final reactions of NO reduction on layered SiC sheet are exothermic. Hence, the barrier of the highest single step should be the overall barrier, i.e., 1.928, 0.722, 1.928, 1.428, and 0.748 eV, respectively, for D_1, D_2, D_3, D_4, and D_5, as shown in Table 2. It is obviously seen from the above discussion that N_2O formation on the layered SiC sheet intrinsically favors the dimer mechanism, in which the layered SiC sheet is more active toward dimeric $(NO)_2$ than toward monomer NO. In particular, the trapezoid $O_{ad}NNO_{ad}$ dimer (D_2) is a necessary intermediate in the energetically most favorable pathway, whose barrier is 0.722 eV. Although the barrier of NO reduction on SiC sheet (0.722 eV) is slightly larger than that of on Si-doped graphene (0.464 eV). However, this kind of metal-free catalyst in our work has two distinct advantages: (1) it has a large active region, making its catalytic activity being fully achieved; (2) layered SiC sheets show more excellent CO tolerance (E_{ad} = −0.080 eV) than Si-doped graphene (E_{ad} = −0.170 eV).

Table 2
The adsorption energies (E_{ad}) of NO monomer, D_1, D_2, D_3, D_4, and D_5 on layered SiC sheet, total energy barrier (E_b), and total reaction energies (E_r) of NO reduction on layered SiC sheets by various pathways for NO reduction. All results are in unit of eV.

Reaction steps	E_{ads}	E_a	E_r
Direction dissociation	−0.118	2.857	0.104
Path I	−1.593	1.928	−2.372
Path II	−0.820	0.722	−2.372
Path III	−0.690	1.928	−2.372
Path IV	−0.487	1.428	−2.372
Path V	−0.478	0.748	−2.372

Since an atomic O is left on the SiC sheet in the process of NO reduction, it is necessary to explore whether this atomic O can be removed by sequent NO molecule. In this process, a NO is initially adsorbed on the O/SiC sheet (Fig. 5a), which is set as the initial state (IS) and the final state (FS) is set as the configuration with NO_2 adsorbed on the SiC sheet (Fig. 5a). The results indicate that the N-atom of NO first attacks to the left O-atom and reaches a transition state. The distance between NO and the O atom is shortened from 2.830 Å of IS to 1.285 Å of TS in this endothermic process, while the distance between the N atom in NO and the Si atom in SiC sheet is elongated from 2.055 Å of IS to 3.819 Å. This transition state is characterized as a NO_2-like species as shown in Fig. 5a, whose energy barrier is about 0.437 eV. Crossing the TS, a NO_2 molecule is formed and it would be released from the SiC sheet due to the weak adsorption of NO_2 on SiC sheet (E_{ads} = −0.198 eV), resulting in the recovery of the layered SiC sheet. Although NO_2 is also harmful,

Please cite this article in press as: J.w. Feng, et al., Layered SiC sheets: A promising metal-free catalyst for NO reduction, J. Mol. Graph. Model. (2015), http://dx.doi.org/10.1016/j.jmgm.2015.05.002

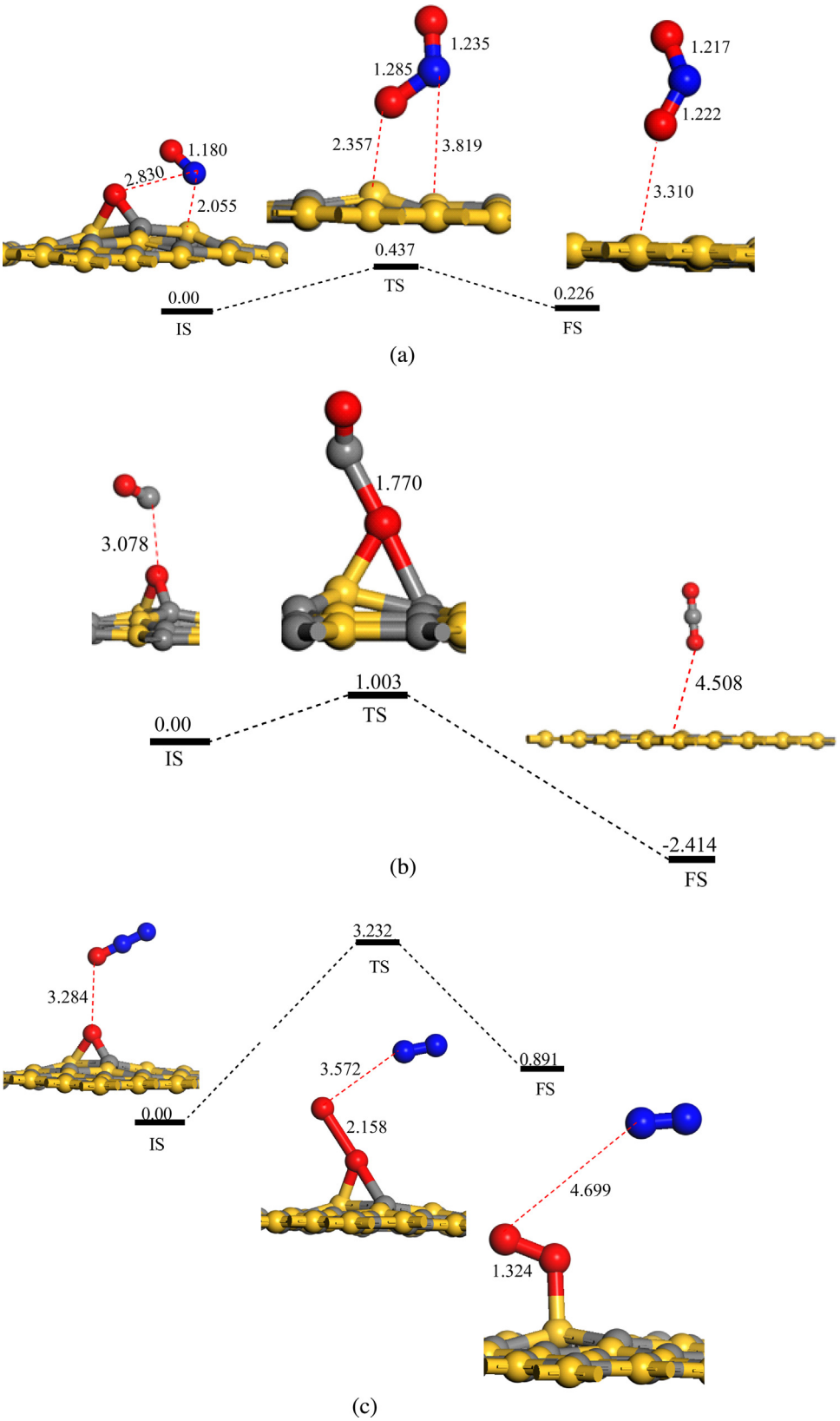

Fig. 5. The MEP profile with the optimized geometries of intermediates, transition states, and products for the recovery of layered SiC sheet by (a) NO, (b) CO, and (c) N_2O molecule. The units of the bond length and energy are Å and eV.

it can be easily captured by water [61], forming useful product, such as H_2NO_3. Furthermore, CO molecule is also a common reactant to remove the left O-atom in NO reduction. Yet, our results indicate that the process of $CO + O \rightarrow CO_2$ has a barrier of 1.003 eV (Fig. 5b), which is higher than that of with NO molecule. In addition, we also consider whether the formed N_2O molecule might pull away the left O atom, forming N_2 and O_2. The results suggest that the barrier of this process is as high as 3.232 eV, indicating that it is

Please cite this article in press as: J.w. Feng, et al., Layered SiC sheets: A promising metal-free catalyst for NO reduction, J. Mol. Graph. Model. (2015), http://dx.doi.org/10.1016/j.jmgm.2015.05.002

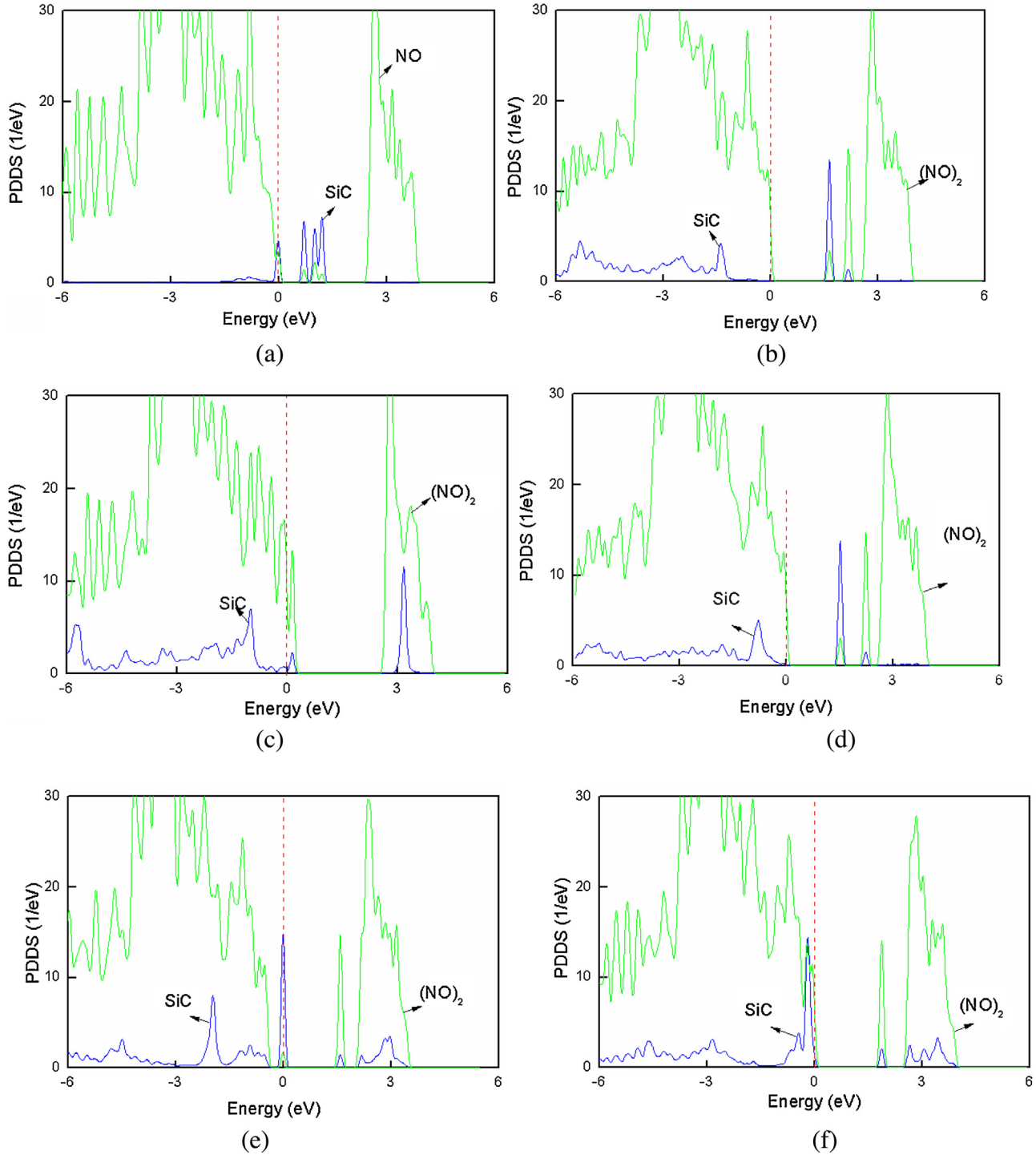

Fig. 6. Calculated projected density of states (PDOS) of (a) NO monomer, (b) D_1, (c) D_2, (d) D_3, (e) D_4, and D_5 on SiC monolayer. The Fermi level has been set to be zero.

kinetically unfavorable. The involved transition state and intermediate are presented in Fig. 5c.

In summary, SiC sheet exhibits good catalytic activity for NO reduction, which can be rationalized by the following reasons: the driving force of the forming dimer $(NO)_2$ on SiC sheet originates from the effective electron transfer from the surface to the dimer, greatly stabilizing the system by the extra electrons on the dimer entering into the N–N bonding orbital. The Hirshfeld charge analysis show that the accumulated net charges on NO and $(NO)_2$ are −0.080, −0.186 (for D_1), −0.379 (for D_2), −0.222 (for D_3), −0.348 (for D_4), and −0.353 *e* (for D_5), respectively, which well consists with the trend of the adsorption energy of these species on layered SiC sheet. As a result, the N—N bond of $(NO)_2$ dimer (1.281, 1.242, 1.357, 1.362, 1.286 Å for D_1, D_2, D_3, D_4, and D_5), is significantly shortened than that of gas phase one (1.970 Å). In other words, when more than NO molecules (such as tetramers) are considered to be reduced on catalysts with high area, they prefer to firstly form some $(NO)_2$ dimers, which are finally converted into N_2. The left atomic O will be removed by NO or CO. The high reactivity of SiC sheet toward NO species can be also observed on the basis of the calculated projected density of states (PDOSs) (Fig. 6). Bonding of $(NO)_2$ to SiC sheet involves the strong hybridization between $2\pi^*$

Please cite this article in press as: J.w. Feng, et al., Layered SiC sheets: A promising metal-free catalyst for NO reduction, J. Mol. Graph. Model. (2015), http://dx.doi.org/10.1016/j.jmgm.2015.05.002

states of $(NO)_2$ (which is unoccupied and located above the Fermi level) and 3p states of Si atom. When $(NO)_2$ is adsorbed on Si-doped grapheme, the $2\pi^*$ components in the PDOS spectra are partly filled and the 3p orbital of Si atom is depopulated. Thus, the catalytic activation of the adsorbed $(NO)_2$ and stretching of the N—O bond can be attributed to the partially occupied antibonding $2\pi^*$ orbital of $(NO)_2$. In addition, we note that the values of PDOSs near the Fermi level of the adsorbed $(NO)_2$ dimers are generally higher than those of NO monomer, which might be a reason that SiC sheet exhibits higher reactivity toward $(NO)_2$ dimer than that of NO monomer.

We should point out that GGA–PBE may be not enough accurate to describe the van der Waal's forces. Using a Grimme approach [62], we take the most favorable pathway as an example to recalculate the configurations of the involved intermediates and transition states. The results indicate that the adsorption energy of D_2 species −1.018 eV, which is larger than that of using pure PBE functional (−0.820 eV). Furthermore, the barrier of this pathway increases to 0.805 eV and the geometric configuration is almost unchanged compared with the result without including the vdW correction. This indicates that the employed methods in the present work can provide qualitatively correct information and remains the popular choice for investigating the mechanisms of some chemical reactions on two-dimensional nanomaterials [44,62–64].

4. Conclusions

By performing DFT calculations, we have investigated the possibility of layered SiC sheet as a metal-free catalyst for NO reduction to N_2O as well as the involved reaction mechanisms. The direct dissociation mechanism is shown to be unfavorable due to the extremely high barrier and endothermicity. In contrast, the catalyzed NO reduction reaction on SiC sheet easily occurs via a dimer mechanism, in which the trapezoid $O_{ad}NNO_{ad}$ species might be a necessary species in the energetically most favorable pathway and the involving barrier is 0.722 eV. Furthermore, we explain the origination of the high catalytic reactivity of SiC sheet on the basis of the calculated charge transfer. The present results suggest that the layered SiC sheets might be a promising metal-free candidate for practical applications in NO reduction.

Acknowledgment

This work is supported by the Scientific Innovation Project for Graduate of Harbin Normal University (HSDSSCX2014-21). The authors would like to show great gratitude to the reviewers for raising invaluable comments and suggestions.

Appendix A. Supplementary data

Supplementary data associated with this article can be found, in the online version, at http://dx.doi.org/10.1016/j.jmgm.2015.05.002

References

[1] G. Bennett, in: B. Bretschneider, J. Kurfurst (Eds.), Air Pollution Control Technology, Elsevier, Amsterdam, The Netherlands, 1986 (ISBN 0-444-98985-4,197, J. Hazard. Mater. 19 (125) (1988)).
[2] F.C. Meunier, J.P. Breen, V. Zuzaniuk, M. Olsson, J.R.H. Ross, Mechanistic aspects of the selective reduction of NO by propene over alumina and silver–alumina catalysts, J. Catal. 187 (1999) 493–505.
[3] R. Burch, J.P. Breen, F.C. Meunier, A review of the selective reduction of NO_x with hydrocarbons under lean-burn conditions with non-zeolitic oxide and platinum group metal catalysts, Appl. Catal. B: Environ. 39 (2002) 283–303.
[4] N. Bogdanchikova, F.C. Meunier, M. Avalos-Borja, J.P. Breen, A. Pestryakov, On the nature of the silver phases of Ag/Al_2O_3 catalysts for reactions involving nitric oxide, Appl. Catal. B: Environ. 36 (2002) 287–297.
[5] A.C. Gluhoi, S.D. Lin, B.E. Nieuwenhuys, The beneficial effect of the addition of base metal oxides to gold catalysts on reactions relevant to air pollution abatement, Catal. Today 90 (2004) 175–181.
[6] S. Roy, A. Baiker, NO_x storage-reduction catalysis: from mechanism and materials properties to storage-reduction performance, Chem. Rev. 109 (2009) 4054–4091.
[7] V. Rosca, M. Duca, M.T. de Groot, M.T.M. Koper, Nitrogen cycle electrocatalysis, Chem. Rev. 109 (2009) 2209–2244.
[8] Y. Hu, K. Griffiths, P.R. Norton, Surface science studies of selective catalytic reduction of NO: progress in the last ten years, Surf. Sci. 603 (2009) 1740–1750.
[9] K. Thirunavukkarasu, K. Thirumoorthy, J. Libuda, C.S. Gopinath, A molecular beam study of the NO + CO reaction on Pd(111) surfaces, J. Phys. Chem. B 109 (2005) 13272–13282.
[10] C.J. Nelin, P.S. Bagus, J. Behm, C.R. Brundle, Core level photoemission of the no dimer: theory and experimental realization for NO/Ag(111), Chem. Phys. Lett. 105 (1984) 58–63.
[11] R.J. Behm, C.R. Brundle, Summary abstract: decomposition of NO on Ag(111) at low temperatures, J. Vac. Sci. 2 (1984) 1040–1041.
[12] A. Ludviksson, C. Huang, H.J. Jänsch, R.M. Martin, Isotopic studies of the reaction of NO on silver surfaces, Surf. Sci. 284 (1993) 328–336.
[13] J.L. Gland, B.A. Sexton, Nitric oxide adsorption on the Pt(111) surface, Surf. Sci. 94 (1980) 355–368.
[14] T.M. Salama, R. Ohnishi, T. Shido, M. Ichikawa, Highly selective catalytic reduction of NO by H_2 over Au^0 and Au(I) impregnated in NaY zeolite catalysts, J. Catal. 162 (1996) 169–178.
[15] A. Ueda, T. Oshima, M. Haruta, Reduction of nitrogen monoxide with propene in the presence of oxygen and moisture over gold supported on metal oxides, Appl. Catal. B: Environ. 12 (1997) 81–93.
[16] M.A.P. Dekkers, M.J. Lippits, B.E. Nieuwenhuys, Supported gold/MO_x catalysts for NO/H_2 and CO/O_2 reactions, Catal. Today 54 (1999) 381–390.
[17] M.A. Debeila, N.J. Coville, M.S. Scurrell, G.R. Hearne, M.J. Witcomb, Effect of pretreatment variables on the reaction of nitric oxide (NO) with Au−TiO_2: DRIFTS studies, J. Phys. Chem. B 108 (2004) 18254–18260.
[18] L. Ilieva, G. Pantaleo, I. Ivanov, R. Nedyalkova, A.M. Venezia, D. Andreeva, NO reduction by CO over gold based on ceria, doped by rare earth metals, Catal. Today 139 (2008) 168–173.
[19] T.D. Chau, T.V. de Bocarme, N. Kruse, Formation of N_2O and $(NO)_2$ during NO adsorption on Au 3D crystals, Catal. Lett. 98 (2004) 85–87.
[20] C.P. Vinod, J.W. Niemantsverdriet Hans, B.E. Nieuwenhuys, Interaction of small molecules with Au clusters: decomposition of NO, Appl. Catal. A: General 291 (2005) 93–97.
[21] J.L.C. Fajín, M.N.D.S. Cordeiro, J.R.B. Gomes, The role of preadsorbed atomic hydrogen in the NO dissociation on a zigzag stepped gold surface: a DFT study, J. Phys. Chem. C 113 (2009) 8864–8877.
[22] Z.P. Liu, P. Hu, CO oxidation and NO reduction on metal surfaces: density functional theory investigations, Top. Catal. 28 (2004) 71–78.
[23] Z.P. Liu, S.J. Jenkins, D.A. King, Step-enhanced selectivity of NO reduction on platinum-group metals, J. Am. Chem. Soc. 125 (2003) 14660–14661.
[24] Z.P. Liu, S.J. Jenkins, D.A. King, Why is silver catalytically active for NO reduction? A unique pathway via an inverted $(NO)_2$ dimer, J. Am. Chem. Soc. 126 (2004) 7336–7340.
[25] Y.Y. Wang, D.J. Zhang, Z.Y. Yu, C.B. Liu, Mechanism of N_2O formation during NO reduction on the Au(111) surface, J. Phys. Chem. C 114 (2010) 2711–2716.
[26] P. Dimick, R. Herman, C. Lyman, A synergistic Pt–Ni catalyst for the reduction of NO with H_2, Catal. Lett. 138 (2010) 148–154.
[27] D.D. Miller, S.S.C. Chuang, Pulse transient responses of NO decomposition and reduction with H_2 on Ag-Pd/Al_2O_3, J. Phys. Chem. C 113 (2009) 14963–14971.
[28] Y. Ji, Y. Luo, First-principles study on the mechanism of photoselective catalytic reduction of NO by NH_3 on anatase TiO_2(101) surface, J. Phys. Chem. C 118 (2014) 6359–6364.
[29] P. Maitarad, J. Han, D.S. Zhang, L.Y. Shi, S. Namuangruk, T. Rungrotmongkol, Structure-activity relationships of NiO on CeO_2 nanorods for the selective catalytic reduction of NO with NH_3: experimental and DFT Studies, J. Phys. Chem. C 118 (2014) 9612–9620.
[30] R.-M. Yuan, G. Fu, X. Xu, H.-L. Wan, Bronsted-NH_4^+ mechanism versus nitrite mechanism: new insight into the selective catalytic reduction of NO by NH_3, Phys. Chem. Chem. Phys. 13 (2011) 453–460.
[31] R. Amrousse, S. El Moumni, A highly distributed Cu_xAu_y-deposited nanotube carbon for selective reduction of NO in the presence of NH_3 at very low temperature, ChemCatChem 6 (2014) 119–122.
[32] X. Wang, Y. Zheng, J. Lin, Highly dispersed Mn–Ce mixed oxides supported on carbon nanotubes for low-temperature NO reduction with NH_3, Catal. Commun. 37 (2013) 96–99.
[33] I. Ellmers, R.P. Vélez, U. Bentrup, A. Brückner, W. Grünert, Oxidation and selective reduction of NO over Fe-ZSM-5: how related are these reactions? J. Catal. 311 (2014) 199–211.
[34] T. Zhang, J. Liu, D. Wang, Z. Zhao, Y. Wei, K. Cheng, et al., Selective catalytic reduction of NO with NH_3 over HZSM-5-supported Fe-sCu nanocomposite catalysts: the Fe–Cu bimetallic effect, Appl. Catal. B: Environ. 148-149 (2014) 520–531.
[35] E. Cruz-Silva, F. Lopez-Urias, E. Munoz-Sandoval, B.G. Sumpter, H. Terrones, J.C. Charlier, et al., Electronic transport and mechanical properties of phosphorus and phosphorus–nitrogen-doped carbon nanotubes, ACS Nano 3 (2009) 1913–1921.

[36] L.P. Zhang, Z.H. Xia, Mechanisms of oxygen reduction reaction on nitrogen-doped graphene for guel cells, J. Phys. Chem. C 115 (2011) 11170–11176.
[37] D. Yu, Q. Zhang, L. Dai, Highly efficient metal-free growth of nitrogen-doped single-walled carbon nanotubes on plasma-etched substrates for oxygen reduction, J. Am. Chem. Soc. 132 (2010) 15127–15129.
[38] Z.-W. Liu, F. Peng, H.-J. Wang, H. Yu, W.-X. Zheng, J. Yang, Phosphorus-doped graphite layers with high electrocatalytic activity for the O_2 reduction in an alkaline medium, Angew. Chem. Int. Ed. 50 (2011) 3257–3261.
[39] K. Gong, F. Du, Z. Xia, M. Durstock, L. Dai, Nitrogen-doped carbon nanotube arrays with high electrocatalytic activity for oxygen reduction, Science 323 (2009) 760–764.
[40] L. Yang, S. Jiang, Y. Zhao, L. Zhu, S. Chen, X. Wang, et al., Boron-doped carbon nanotubes as metal-free electrocatalysts for the oxygen reduction reaction, Angew. Chem. Int. Ed. 50 (2011) 7132–7135.
[41] Z. Yang, Z. Yao, G. Li, G. Fang, H. Nie, Z. Liu, et al., Sulfur-doped graphene as an efficient metal-free cathode catalyst for oxygen reduction, ACS Nano 6 (2012) 205–211.
[42] X. Sun, P. Song, Y. Zhang, C. Liu, W. Xu, W. Xing, A class of high performance metal-free oxygen reduction electrocatalysts based on cheap carbon blacks, Sci. Rep. 3 (2013) 2505.
[43] Y. Zhang, J. Ge, L. Wang, D. Wang, F. Ding, X. Tao, et al., Manageable N-doped graphene for high performance oxygen reduction reaction, Sci. Rep. 3 (2013) 2771.
[44] J.X. Zhao, Y. Chen, H.G. Fu, Si-embedded graphene: an efficient and metal-free catalyst for CO oxidation by N_2O or O_2, Theor. Chem. Acc. 131 (2012) 11.
[45] Y. Chen, Y.-J. Liu, H.-X. Wang, J.-X. Zhao, Q.-H. Cai, X.-Z. Wang, et al., Silicon-doped graphene: an effective and metal-free catalyst for NO reduction to N_2O? ACS Appl. Mater. Interfaces 5 (2013) 5994–6000.
[46] L. Sun, Y. Li, Z. Li, Q. Li, Z. Zhou, Z. Chen, et al., Electronic structures of SiC nanoribbons, J. Chem. Phys. 129 (2008) 174114.
[47] Y. Jing, Z. Zhou, C.R. Cabrera, Z. Chen, Graphene, inorganic graphene analogs and their composites for lithium ion batteries, J. Mater. Chem. A 2 (2014) 12104–12122.
[48] Q. Tang, Z. Zhou, Graphene-analogous low-dimensional materials, Prog. Mater. Sci. 58 (2013) 1244–1315.
[49] Y. Li, F. Li, Z. Zhou, Z. Chen, SiC_2 silagraphene and its one-dimensional derivatives: where planar tetracoordinate silicon happens, J. Am. Chem. Soc. 133 (2011) 900–908.
[50] P. Zhang, B.B. Xiao, X.L. Hou, Y.F. Zhu, Q. Jiang, Layered SiC sheets: a potential catalyst for oxygen reduction reaction, Sci. Rep. 4 (2014) 8.
[51] P. Jamet, S. Dimitrijev, P. Tanner, Effects of nitridation in gate oxides grown on 4H-SiC, J. Appl. Phys. 90 (2001) 5058–5063.
[52] B. Delley, An all-electron numerical method for solving the local density functional for polyatomic molecules, J. Chem. Phys. 92 (1990) 508–517.
[53] B. Delley, From molecules to solids with the DMol3 approach, J. Chem. Phys. 113 (2000) 7756–7764.
[54] J.P. Perdew, K. Burke, M. Ernzerhof, Generalized gradient approximation made simple, Phys. Rev. Lett. 77 (1996) 3865–3868.
[55] F.L. Hirshfeld, Bonded-atom fragments for describing molecular charge densities, Theor. Chim. Acta 44 (1977) 129–138.
[56] G. Henkelman, H. Jónsson, Improved tangent estimate in the nudged elastic band method for finding minimum energy paths and saddle points, J. Chem. Phys. 113 (2000) 9978–9985.
[57] S.K. So, R. Franchy, W. Ho, The adsorption and reactions of NO on Ag(111) at 80 K, J. Chem. Phys. 91 (1989) 5701–5706.
[58] S.K. So, R. Franchy, W. Ho, Photodesorption of NO from Ag(111) and Cu(111), J. Chem. Phys. 95 (1991) 1385–1399.
[59] B.E. Hayden, An infra-red reflection absorption study of the adsorption of NO on Pt(111), Surf. Sci. 131 (1983) 419–432.
[60] C.E. Dinerman, G.E. Ewing, Infrared spectrum, structure, and heat of formation of gaseous $(NO)_2$, J. Chem. Phys. 53 (1970) 626–631.
[61] X. Zhang, Z. Lu, Y. Tang, D. Ma, Z. Yang, Depletion NO_x made easy by nitrogen doped graphene, Catal. Lett. 144 (2014) 1016–1022.
[62] Y.-H. Lu, M. Zhou, C. Zhang, Y.-P. Feng, Metal-embedded graphene: a possible catalyst with high activity, J. Phys. Chem. C 113 (2009) 20156–20160.
[63] Y. Li, Z. Zhou, G. Yu, W. Chen, Z. Chen, CO catalytic oxidation on iron-embedded graphene: computational quest for low-cost nanocatalysts, J. Phys. Chem. C 114 (2010) 6250–6254.
[64] E.H. Song, Z. Wen, Q. Jiang, CO catalytic oxidation on copper-embedded graphene, J. Phys. Chem. C 115 (2011) 3678–3683.

Please cite this article in press as: J.w. Feng, et al., Layered SiC sheets: A promising metal-free catalyst for NO reduction, J. Mol. Graph. Model. (2015), http://dx.doi.org/10.1016/j.jmgm.2015.05.002